Molecular dynamics averaging of Xe chemical shifts in liquids

Cynthia J. Jameson and Devin N. Sears
Department of Chemistry, MC-111, University of Illinois at Chicago, Chicago, Illinois 60607-7061

Sohail Murad
Department of Chemical Engineering, University of Illinois at Chicago, Chicago, Illinois 60607

(Received 22 July 2004; accepted 26 August 2004)

The Xe nuclear magnetic resonance chemical shift differences that afford the discrimination between various biological environments are of current interest for biosensor applications and medical diagnostic purposes. In many such environments the Xe signal appears close to that in water. We calculate average Xe chemical shifts (relative to the free Xe atom) in solution in eleven liquids: water, *iso*butane, perfluoro-*iso*butane, *n*-butane, *n*-pentane, neopentane, perfluoroneopentane, *n*-hexane, *n*-octane, *n*-perfluorooctane, and perfluorooctyl bromide. The latter is a liquid used for intravenous Xe delivery. We calculate quantum mechanically the Xe shielding response in Xe-molecule van der Waals complexes, from which calculations we develop Xe (atomic site) interpolating functions that reproduce the *ab initio* Xe shielding response in the complex. By assuming additivity, these Xe-site shielding functions can be used to calculate the shielding for any configuration of such molecules around Xe. The averaging over configurations is done via molecular dynamics (MD). The simulations were carried out using a MD technique that one of us had developed previously for the simulation of Henry's constants of gases dissolved in liquids. It is based on separating a gaseous compartment in the MD system from the solvent using a semipermeable membrane that is permeable only to the gas molecules. We reproduce the experimental trends in the Xe chemical shifts in *n*-alkanes with increasing number of carbons and the large chemical shift difference between Xe in water and in perfluorooctyl bromide. We also reproduce the trend for a given solvent of decreasing Xe chemical shift with increasing temperature. We predict chemical shift differences between Xe in alkanes vs their perfluoro counterparts.
 [DOI: 10.1063/1.1807817]

I. INTRODUCTION

Optical pumping methods are being used to achieve nonequilibrium nuclear spin polarization in the noble gases ^{3}He and ^{129}Xe. The enhanced signal of such hyperpolarized gases in nuclear magnetic resonance (NMR) has been utilized in biomedical imaging of void spaces, including investigation of healthy and diseased human lungs *in vivo*.[1,2] Hyperpolarized xenon introduced into blood or tissues provides *in vivo* chemical shift-selective imaging for investigations. Xenon may have an inherent advantage for such investigations because it is ≈15–20 times more soluble in blood and tissue than helium, and is preferentially incorporated into lipid-containing and protein-containing components. Tissue-dissolved hyperpolarized Xe NMR signals from the thorax and from brain have already been observed in both rodents and humans, and Xe images were recorded from the brain of a live rat using two-dimensional chemical shift imaging.[3] One drawback of the use of Xe in humans is that it is an anaesthetic.

Dissolving hyperpolarized xenon gas in a liquid for subsequent injection into the organism was suggested by Bifone *et al.*[4] Intravenous injection of xenon dissolved in a bolus of a biocompatible liquid is a far more promising method than inhalation of the gas for maintaining the polarization during introduction of the xenon to blood and tissues. Saline solutions had been used, but xenon has a limited solubility in water. The high solubility of Xe in perfluorocarbons, the long Xe T_1 relaxation time of dissolved gas, and the chemical and biological inertness of these liquids suggest their use for delivery of hyperpolarized xenon. Perfluorocarbon-based emulsions have been designed for use as blood substitutes. These biocompatible emulsions contain perfluorocarbon droplets that are stabilized by a phospholipid monolayer. The droplet size is small enough to pass through the lung capillaries. These properties suggest a perfluorocarbon emulsion as an intravenous delivery medium for hyperpolarized xenon. Bifone and co-workers demonstrated that the perfluorooctyl bromide emulsions with droplet sizes $\geqslant 5$ μm have the narrow Xe NMR lines that would permit the use of perfluorooctylbromide (PFOB) emulsions as delivery media for hyperpolarized xenon *in vivo*.[5] Subsequently, Bifone and co-workers have used this delivery medium to carry out *in vivo* hyperpolarized Xe NMR spectroscopy in tumors and to study blood oxygenation. The chemical shift of a xenon atom in aqueous solution is 196 ppm and in perfluorooctyl bromide it is 106 ppm.[5] The very large differences in intermolecular chemical shift typical of the xenon atom is the major advantage in discrimination of Xe signals from blood and various tissues,[3] and in discrimination of Xe signals in healthy and cancerous tissues.[6] The Xe chemical shift differences that afford this fine discrimination are therefore of great interest for diagnostic purposes.

Xe is soluble in organic solvents in which it has a chemical shift range from 85 ppm (in hexafluorobenzene) to 246.7 ppm (in iodobenzene),[7] relative to free Xe atom. The significant body of experimental data of Xe in liquids has been largely due to the work of Stengle and Williamson,[8–12] with later additions from Lim and King.[13,14] More recent data including alkyl alcohols, ketones, and acids have been provided by Luhmer and Bartik.[15] Lim and King[13,14] as well as Luhmer and Bartik[15] have proposed empirical models of group contributions based on the Xe chemical shift dependence on number of carbons in the solvent molecule. These models suggested that the Xe chemical shift increases linearly with fraction of CH_2 groups.[13,14] Bonifacio and Filipe have suggested that all such analyses are flawed which do not take into account the fact that the solvents in which the Xe shifts are dissolved are not in the same thermodynamic states at the same temperature.[16] Therefore, these authors have made measurements of Xe chemical shifts in solutions as a function of temperature and they suggest that valid comparisons could be made for solvents at the same reduced temperature, or at the same mass density, in order to compare Xe in solvents at the same thermodynamic state. In such comparisons, the Xe chemical shifts are found to actually decrease with increasing fraction of CH_2, and decrease with increasing number of C atoms.[16] Experimentally, Xe chemical shifts in solution decrease with increasing temperature for the same organic solvent.[8,16]

Previous treatments of Xe chemical shifts in solution have been entirely empirical. The models used were based on the reaction field theory of Onsager which describes the liquid as a continuum. Linear correlations of the Xe chemical shifts with a function of the refractive index of the pure solvent $f(n)=[(n^2-1)/(2n^2+1)]^2$, for example, have been found for liquids of similar molecular types. The use of this function, based on the idea that the major chemical shift contribution arises from the dispersive part of the van der Waals interactions, was suggested by Rummens.[17,18] The more recent interpretations by Luhmer and Bartik are still based on dispersion contributions as the primary origin of Xe chemical shifts in the various solvents, differing from the Rummens model in that the Xe chemical shifts are assumed directly proportional to the Xe-solvent dispersion energy, where the latter is taken from a PISA (pair interaction structureless approximation) model.[15,19,20] These models involve primarily parameter fitting and do not permit calculations of the Xe chemical shifts from first principles. They provide no satisfactory explanation either for the nonzero intercept in the linear fit or the way in which such intercepts change with solvent molecule type.

In this paper, we offer the first theoretical calculations of chemical shifts for Xe atoms dissolved in liquid solvents by using quantum mechanically calculated shielding response functions in classical atomistic molecular dynamics simulations. We investigate the large experimentally observed difference in Xe chemical shifts between xenon dissolved in water and Xe in perfluorooctyl bromide, a liquid used for intravenous Xe delivery. We also systematically investigate Xe dissolved in *n*-alkanes, in which the Xe chemical shifts have been measured as a function of temperature.[8,16] We calculate average Xe chemical shifts (relative to the free Xe atom) in solution in eleven liquids: water, *iso*-butane, perfluoro-*iso*butane, *n*-butane, *n*-pentane, neopentane, perfluoroneopentane, *n*-hexane, *n*-octane, *n*-perfluorooctane, and perfluorooctyl bromide.

Our goal is to provide a fundamental understanding of the Xe chemical shift in liquid solvents that goes beyond empirical correlations with bulk properties such as refractive index. Quantum mechanical calculations have already shown that, although electron correlation can have a significant contribution, the dominant part of the Xe intermolecular shielding response can be found at the self-consistent-field (SCF) level,[21–23] without including electron correlation. This finding is at odds with the use of dispersion-based models that have dominated the literature on Xe chemical shifts in solution.[8,17] In addition, we seek to understand the ways in which the liquid structure of the solvent plays a role in the Xe chemical shifts in solution.

II. METHODS

A. Approach

In order to develop an understanding of Xe chemical shifts in liquid solvents, we adopt an approach that eliminates any need for adjustable parameters. We use the same approach as for Xe in the gas phase and for Xe occluded in cages and channels in the crystalline phase. The Xe atom has an intrinsic shielding response in a particular configuration of neighbors. This is an electronic property which can be described by quantum mechanical calculations. The probabilities of system configurations, on the other hand, can be described by a statistical mechanical calculation using integrations, or grand canonical Monte Carlo or classical molecular dynamics simulations. For the present work, we assume transferability, i.e., we import directly those potential functions and shielding response functions, which have been tested against either gas phase data (Xe in CH_4 and CF_4), or data in the crystalline solid (Xe in water cages in clathrate hydrates) for use in the molecular dynamics simulations. That is, we assume that the electronic factors are preserved (same interaction potential energy functions and same shielding functions), and that the only difference between the previous systems and the systems of Xe in liquid solvents arises from the probability distributions of system configurations. To provide the latter, we use molecular dynamics simulations methods and liquid-liquid potentials that have been successfully employed for simulations of liquid properties.

B. Chemical shift functions

The observed chemical shift in solution arises from the difference in shielding between the free Xe atom (the reference) and the isotropic shielding of Xe dissolved in solution. Although the observed Xe chemical shift δ is related to the shielding by

$$\delta=[\sigma_{(\text{free Xe atom})}-\sigma_{(\text{Xe in sample})}]/[1-\sigma_{(\text{free Xe atom})}],$$

when we neglect the absolute shielding of the free Xe atom itself compared to 1.0, the Xe chemical shift δ observed in solution is given by

$$\delta \approx \sigma_{(\text{free Xe atom})} - \sigma_{\text{iso}(\text{Xe in infinitely dilute solution in a spherical sample})}. \quad (1)$$

In what follows, we will use the term Xe chemical shift functions, rather than shielding response functions, having already expressed the results of shielding calculations with respect to the free Xe atom.

In a separate study of the chemical shifts of Xe in the small and large cages of clathrate hydrate structure I and II, we have determined the Xe tensor in large basis set quantum mechanical calculations, using density functional theory, for Xe atom in cages of water molecules. In that study we obtained Xe shielding contributions from O atoms as a function of the Xe–O distance, and Xe shielding contributions from H atoms as a function of the Xe–H distance. These functions had been used to calculate average chemical shifts using Monte Carlo simulations in 12 different water cages in crystal fragments.[24,25] The chemical shift function is expressed as follows:

$$\delta = \sum_{\mathrm{O}(j)} \sum_{n=6}^{12} o_n r_{\mathrm{Xe-O}(j)}^{-n} + \sum_{\mathrm{H}(k)} \sum_{n=6}^{12} h_n r_{\mathrm{Xe-H}(k)}^{-n}. \quad (2)$$

Equation (2) is obtained directly from the functions that were fitted to the quantum mechanical values for Xe in water cages of known structure. In this way it represents the actual quantum mechanical values for Xe in a particular position within a cage within a crystal of water molecules. The site-site additive form is merely a convenience and, in this case, permits direct application to Xe surrounded by water molecules in arbitrary configurations. That is, the functions $\Sigma_{n=6}^{12} o_n r_{\mathrm{Xe-O}}^{-n}$ and $\Sigma_{n=6}^{12} h_n r_{\mathrm{Xe-H}}^{-n}$ taken together, may be considered as the universal chemical shift functions for Xe in the presence of neighboring H_2O molecules. The parameters Q_n and h_n were obtained by fitting quantum mechanical values of shielding (relative to free Xe atom) for Xe in 73 different configurations involving 40–48 explicit water molecules in a crystal fragment represented by periodic point charge arrays providing the proper Madelung potential at the Xe position, using large basis sets in all-electron calculations, especially for the Xe atom for which 240 basis functions were used. These crystalline systems are clathrate hydrates in which the coordinates of oxygen and hydrogen atoms that constitute the cages of water molecules which form around the Xe atoms are well established from neutron diffraction studies. Since the same set of functions predicted the isotropic Xe chemical shifts in twelve distinct types of cages in clathrate hydrates, we believe that these functions can be considered as universal shielding functions for Xe interacting with water.[24] The universality of these Xe–O and Xe–H chemical shift functions has been established by accurate predictions of Xe chemical shifts in twelve types of clathrate hydrate cages from quantum mechanical calculations in only two types of cages.[24,25] In this paper, we use these same sets of chemical shift functions for molecular dynamic simulations of Xe dissolved in water in order to obtain the Xe chemical shift in aqueous solution.

TABLE I. Investigation of the electronic factors as a function of distance between Xe and the closest C atom. Values given are δ_{iso}/ppm $= \sigma(\text{free Xe atom}) - \sigma(\text{Xe,model})$ for the Xe isotropic shielding calculated in vacuum for model systems, with the Xe approach normal to the plane of the three H atoms in H_3C.

r(Xe–C) (Å)	Xe@H_3CH	Xe@H_3CCH_3	Difference
3.5	66.60	63.06	3.54
4.0	21.31	20.09	1.22
4.5	6.23	5.86	0.37
5.0	1.67	1.58	0.09

The Xe@CH_4 shielding response functions are not entirely transferable to Xe@C_nH_{2n+2}. The electronic structure of the C and H atoms within C_nH_{2n+2} is different from that in CH_4, thus eliciting a somewhat different Xe shielding response per C and per H. An indication of the magnitude of the expected deviations arising from this is given in Table I, where replacement of one H atom in CH_4 by a CH_3 group results in a lower Xe chemical shift. Therefore, our simulations for Xe in alkanes should overestimate the Xe chemical shift by at least 5%. The fractional change would increase upon substitution of another H atom by a CH_3 group.

In a separate study, we have determined the Xe–C(H), Xe–C(F), Xe–H, and Xe–F shielding functions for Xe interacting with CH_4 or CF_4 molecule from quantum mechanical calculations of Xe shielding in $XeCH_4$ and $XeCF_4$ supermolecules.[23] These shielding functions, relative to the free Xe atom, were used to predict the Xe chemical shifts in mixtures of Xe and CH_4 and of Xe and CF_4 gases in the limit of very low Xe mole fraction, as a function of CH_4 or CF_4 density and temperature.[26] We will use the Xe–C(H), Xe–C(F), Xe–H, and Xe–F chemical shift functions so obtained, for the calculations of Xe chemical shifts for Xe dissolved in *any* liquid hydrocarbon or perfluorocarbon. Thus, for Xe in liquid alkanes, the Xe chemical shift function is expressed as

$$\delta = \sum_{\mathrm{H}(j)} \sum_{n=6}^{14} h_n r_{\mathrm{Xe-H}(j)}^{-n} + \sum_{\mathrm{C}(k)} \sum_{n=6}^{14} c_n r_{\mathrm{Xe-C}(k)}^{-n} \quad (3)$$

with the coefficients transferred directly from the Xe@CH_4 system. An analogous equation is used for the averaging of Xe chemical shifts in liquid perfluoroalkanes using Xe–F and Xe–C(F) chemical shift functions taken directly from the Xe@CF_4 system.

For the averaging of Xe chemical shifts in liquid $CF_3(CF_2)_6CF_2Br$, the Xe chemical shift in liquid PFOB was treated as a pairwise sum of three Xe-site chemical shift functions: Xe–F, Xe–Br, and Xe–C, where the Xe–C and Xe–F functions were taken from the Xe@CF_4 system. The Xe–Br chemical shift function was obtained by scaling the Xe–F chemical shift to Xe–Br chemical shift using well known scaling procedures.[27] Thus, for Xe in liquid perfluorooctylbromide, the Xe chemical shift is expressed as

TABLE II. Coefficients for site-site isotropic chemical shift functions used in Eqs. (2)–(4) in this work.

n	6	8	10	12	14
Xe–C(H_n), c_n ($Å^{-n}$)	$-1.482\,11\times10^5$	$1.045\,90\times10^7$	$-1.901\,32\times10^8$	$1.384\,33\times10^9$	$-3.455\,61\times10^9$
Xe–C(F_n), c_n ($Å^{-n}$)	$-1.628\,91\times10^4$	$2.909\,18\times10^6$	$-4.835\,19\times10^7$	$2.760\,70\times10^8$	$-5.230\,79\times10^8$
Xe–H, h_n ($Å^{-n}$)	$8.583\,34\times10^3$	$-6.557\,33\times10^5$	$1.421\,31\times10^7$	$-6.347\,47\times10^7$	$4.200\,88\times10^7$
Xe–F, f_n ($Å^{-n}$)	$7.445\,68\times10^3$	$-6.937\,67\times10^5$	$1.899\,30\times10^7$	$-1.321\,48\times10^8$	$2.776\,10\times10^8$
Xe–Br, b_n ($Å^{-n}$)	$6.151\,51\times10^4$	$-6.678\,64\times10^6$	$2.130\,42\times10^8$	$-1.727\,15\times10^9$	$4.227\,67\times10^9$
Xe–O_{water}, o_n ($Å^{-n}$)	$-1.368\,40\times10^4$	$7.146\,288\times10^5$	$-2.042\,105\times10^6$	$-5.850\,74\times10^6$	0.0
Xe–H_{water}, h_n ($Å^{-n}$)	$-7.738\,67\times10^2$	$1.167\,619\times10^5$	$-5.820\,547\times10^5$	$7.143\,563\times10^5$	0.0

$$\delta=\sum_{F(j)}\sum_{n=6}^{14} f_n r_{Xe-F(j)}^{-n}+\sum_{C(k)}\sum_{n=6}^{14} c_n r_{Xe-C(k)}^{-n}+\sum_{Br(l)}\sum_{n=6}^{14} b_n r_{Xe-Br(l)}^{-n}, \quad (4)$$

where the outside sums are over all the F, C, and Br atoms in the simulation box within the cutoff distance from the Xe atom, under periodic boundary conditions. In all cases, the pairwise chemical shift functions had been constrained to approach the free Xe atom limit, zero, so as to match the limiting behavior calculated in the supermolecule.[23] Thus, each of the Xe chemical shift functions have typically gone to zero at much shorter distances than the cutoff distance used in the MD simulation box. The parameters in Eqs. (2)–(4) are given in Table II.

C. Molecular dynamics

The averaging to obtain Xe chemical shifts can be carried out in various ways. In this paper, we employ a molecular dynamics-based method using an algorithm developed by one of us to study the solubility of gases in liquids. The method has been described in previous publications[28,29] so we will only summarize it here. The simulation box consists of a solvent/solution compartment separated from the gas compartment by a semipermeable membrane. A schematic diagram of the simulation system is shown in Fig. 1. Periodic boundary conditions then lead to a system infinite in the y and z directions (parallel to the membranes). In the x direction this leads to alternating gas and solvent sections of width $L_x/2$ (L_x is the system size in the x direction, i.e., perpendicular to the membranes). In this method, the membrane typically consists of several layers of atoms arranged in a fcc configuration. In the present study the membrane simply consisted of a single layer of atoms. The membrane is formed by tethering the atoms that constitute the membrane to their equilibrium positions with a simple harmonic potential, although other potentials could also be used. For the present application, the membrane atoms are fictitious; the membrane serves as a means of including all parts of the equilibrium system (the gas and the solution) in the simulation box. The membrane is made permeable to the gas molecules but not to the solvent molecules. This has been accomplished for these studies by adjusting the pore size of the membrane, and adjusting the intermolecular interaction between the solvent or gas molecules and the membrane.[29]

The density and temperature of the solution compartment can be fixed to correspond to the state condition of interest. In this study, the density of the liquid phase was set equal to the experimental density of the solvent at the temperature of interest. This establishes the volume of the solution compartment once the number of solvent molecules to be included in the solution compartment is fixed. In these simulations, the solution compartment consisted of typically 480 solvent and solute molecules and the two membrane walls were constructed of 64 atoms. The number of Xe atoms found in the solution compartment is typically small. Since the simulations for averaging the Xe chemical shifts are carried out to mimic the solution at infinite dilution in Xe, the Xe–Xe contributions to the Xe chemical shift in the solution compartment are not included. They are similarly ignored in the gas compartment. The volume of the gas compartment has been set to be equal to the solvent compartment (although this is not essential). In the initial setup the gas compartment would have as many Xe atoms as to give the gas any desired density/pressure. The gas compartment typically starts out with 40–80 atoms of xenon in the simulations for which results are shown here. The length of the simulation system perpendicular to the membrane has been set to four times that parallel to the membrane. Furthermore, the lengths parallel to the membrane were set to be the same ($L_y=L_z$). These relative dimensions minimize the effect of the membrane on the overall system.

An important advantage of setting the solvent density

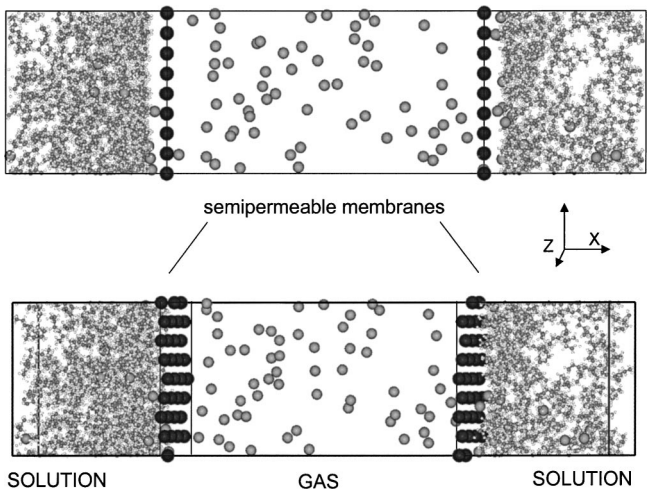

FIG. 1. The basic simulation system for investigating chemical shift and solubility of gases dissolved in liquids.

equal to the experimental density of the pure solvent in the MD simulation at the temperature of interest is as follows. The average Xe chemical shift is extremely sensitive to the effective free volume in the solvent, and a MD simulation that permits either the volume or the number of solvent molecules to vary would not provide the correct free volume for the Xe unless the solvent-solvent potentials were extremely accurate. Since the total number of solvent molecules remains fixed during the simulation and is at least an order of magnitude as large as the equilibrium number of Xe atoms in the solution, the average liquid density in the solution compartment remains very nearly constant throughout the simulation.

The molecules were given a Gaussian velocity distribution corresponding to the system temperature being investigated. The time evolution of this initial system setup was then followed using a fifth order predictor-corrector scheme for the translational motion and a fourth order predictor scheme using quaternions for the rotational motion.[30] The temperature was held constant using a Gaussian thermostat. The simulation system was allowed to equilibrate for $6\times10^4-1\times10^5$ time steps. After this, production runs were carried out for $5\times10^5-1\times10^6$ time steps, each of size 2×10^{-16} s for water and 4×10^{-16} s for hydrocarbons. Some simulations, where we calculated the Henry's constant were up to 3×10^6 steps.

Typically, the initial system configuration consists of a solution section with 15–40 atoms of xenon and 440–465 molecules of solvent, for example. Equilibrium is obtained more rapidly for systems with very low Xe solubility (such as water) if the solution has an excess of xenon, since expulsion of xenon from such solutions is more rapid than diffusion of xenon into the solution from the gas phase. The solubility of Xe in water is very low,[31] while that of Xe in organic liquids is much higher.[32–34] For Xe in organic liquids this does not appear to be a problem.

After the initial equilibration run, the simulation is continued in which the Xe chemical shift is calculated every time step for each Xe atom and the averages calculated over all Xe atoms every 10 000–20 000 steps, using the chemical shift functions shown in the appropriate one of Eqs. (2)–(4). To ensure that only xenon atoms completely surrounded by solvent molecules were included in this sum (i.e., to exclude xenon molecules near the membranes for the purpose of averaging the properties of xenon atoms in the solution), only those xenon atoms in the middle half of the solution compartment (see Fig. 1) were included in accumulating the sums in Eqs. (2)–(4). Typical density profiles of Xe and solvent in the simulation system are shown in Fig. 2. In our preliminary studies, we had found early convergence of the chemical shift average in comparison to solubility or Henry's law constant.[35] We find this to be the case in the present work for all the liquids. In most runs, the chemical shift averages converged within 1×10^5 (2×10^5 in a few cases) time steps. For Henry's constant (solubility), convergence required between 5×10^5 and 3×10^6 time steps.

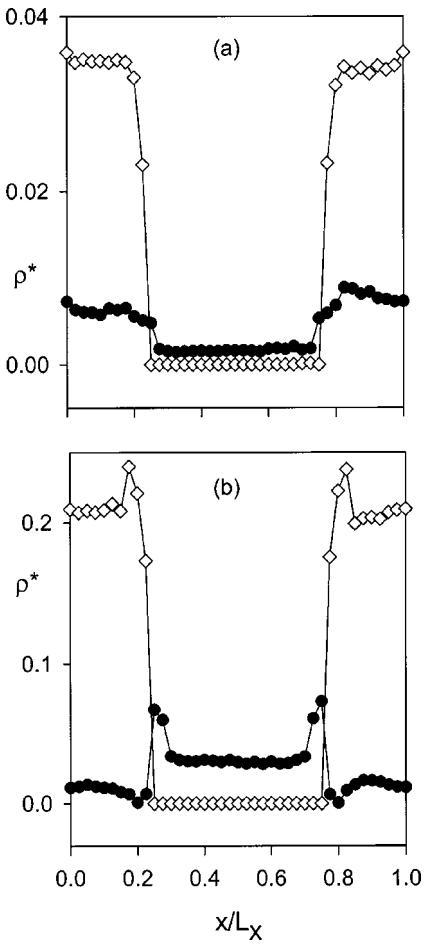

FIG. 2. The density profiles of solvent and Xe at the end of a typical MD simulation with 10^6 steps. Here ρ^* represents the reduced number density, ρr_0^3. Filled circles correspond to Xe and the open symbols are (a) *n*-butane, (b) water. The two membranes are at $x=0.25L_x$ and $0.75L_x$.

D. Potential functions

We adopt for Xe in the alkanes and perfluoroalkanes the same set of pairwise potentials that have been tested against the measurements of the Xe chemical shift in $Xe-CH_4$ and $Xe-CF_4$ gas mixtures as a function of temperature and for chemical shifts in $Xe-CH_4$ mixtures in zeolites.[23,36] The Aziz Xe–Kr potential function,[37] fitted to an exp-6 form, was adopted for Xe–Br. For the $Xe-H_2O$ potential we adopt the same potential as was used for the calculation of the Xe chemical shifts in clathrate hydrates.[24,25] For the present work, we use an exp-6 fit rather than the Maitland-Smith form, since the former is more convenient to use in molecular dynamics codes:

$$u_{\mathrm{Xe}-i}=\sum_i \epsilon_{\mathrm{Xe}i}\left\{\left(\frac{6}{\alpha_{\mathrm{Xe}i}-6}\right)\exp[\alpha_{\mathrm{Xe}i}(1-\bar{r})]-\left(\frac{\alpha_{\mathrm{Xe}i}}{\alpha_{\mathrm{Xe}i}-6}\right)\bar{r}^{-6}\right\}, \tag{5}$$

where $\bar{r}=r_{\mathrm{Xe}i}/r_{\mathrm{min,Xe}i}$. The parameters ϵ, α, and r_{min} for $Xe-C_{\mathrm{alkyl}}$, $Xe-H_{\mathrm{alkyl}}$, Xe–F, and Xe–Br are given in Table III.

TABLE III. Site-site potential functions used in Eq. (5) in this work. Original sources for the functions are given in the text. $V(R_{XeA})=\epsilon\{(6/\alpha-6)\exp[\alpha(1-\bar{r})]-(\alpha/\alpha-6)\bar{r}^{-6}\}$.

	ϵ/k_B (K)	α	r_{min} (Å)
Xe–C(H_4)	141.2	16.1	3.99
Xe–C(F_4)	141.2	16.1	3.99
Xe–H_{alkyl}	53.3	15.9	3.66
Xe–F	78.5	14.2	3.93
Xe–Br	233.0	17.0	4.17
Xe–O_{water}	105.0	15.2	3.74
Xe–H_{water}	73.1	14.2	3.47

TABLE IV. Lennard-Jones parameters for the solvent-solvent potentials used in this work.

	ϵ/k_B (K)	r_0 (Å)	Reference
C–C	25–73[a]	3.80–3.96[a]	41
F–C	48	3.54	b
Br–C	141	3.76	b
F–F	31	3.12	30
Br–Br	271	3.56	30
Br–F	92	3.34	b

[a]Includes attached H atoms for hydrocarbons ($CH_n\cdots CH_n$ interactions). Actual values used for various CH_n types are given in Table III of Ref. 41.
[b]Estimated using Lorenz-Berthelot rules (Ref. 30).

The Xe–Xe chemical shift contributions are not included in the averaging, thereby resulting in an average appropriate to the infinite dilution limit. The Xe–Xe potential and chemical shift functions are irrelevant to the calculations of Xe chemical shifts in this study since measurements had been made in very dilute solutions of Xe.

Potential functions used recently in MD simulations of liquid perfluoroalkanes modeled them as chains of tangentially bonded spherical segments of hard-core diameter sigma, and the attractive interactions described by square well potentials.[38] In other studies, the AMBER5 potential functions have been used for perfluorinated decane, for example.[39] In the present work, we used the OPLS-AA (optimized potentials for liquid simulations, all-atom) model;[42] that is, the perfluoroalkane molecules are treated atomistically, but internal rotation about the C–C bonds is not permitted. The potential models adopted for the solvent-solvent interactions are of the form

$$u=\sum_{i,j} 4\epsilon_{ij}\left[\left(\frac{r_{ij}}{\sigma_{ij}}\right)^{-12}-\left(\frac{r_{ij}}{\sigma_{ij}}\right)^{-6}\right]+q_iq_j/r_{ij}, \tag{6}$$

where ϵ and σ are the Lennard-Jones energy and size parameters, q the charge, i and j the active sites, while r_{ij} is the distance between the active sites i and j. These potential models are known to give a reasonable quantitative picture of a wide range of thermodynamic properties of liquids.[40] Potential parameters used in the present work are given in Table IV.

The partial charges of the alkanes and perfluoroalkanes were obtained from DFT/B3LYP calculations of the solvent molecule in vacuum using the 6-31G* basis set. These (Löwdin) charges were used only in the solvent-solvent interactions, and their absolute magnitudes have influence on the averaging of the Xe chemical shift only by their effects on the free volumes afforded to Xe atom in the liquid solvent.

For the MD simulations in the alkanes, the solvent-solvent potentials used the same parameters (ϵ and σ) as in the OPLS model,[41] but no internal rotation was permitted, and we used the rigid all-trans configurations for the carbon backbone. Here, in keeping with the OPLS model for the purposes of calculating solvent-solvent interactions, hydrogens on carbon are implicit and the interaction sites for the CH_n groups are neutral and centered on the carbons. The Xe–H interactions are explicitly included, however, with the proton positions at their normal bond lengths and bond angles.

For the MD simulations in liquid water, we have tested two widely used potential models, the SPC (simple point charge) model and the TIP4P (transferable intermolecular potential functions, 4-point) model. Both these potentials can reproduce the density of water as a function of temperature.[43] The SPC model has acceptable agreement while the TIP4P has good agreement with the structure of liquid water. A recent review of liquid water potentials by Guillot provides a comprehensive assessment of the current state of the art in computer simulations of liquid water.[44]

III. RESULTS

The present work provides MD simulations of Xe chemical shifts for Xe atoms in liquid solvents. Previous MD simulations carried out for Xe in liquids addressed relaxation mechanisms (dipolar and quadrupolar relaxation).[45–49]

The bulk susceptibility contributions are sample-shape-dependent and are not included in our simulations. Thus, comparisons have to be made with experimental data which have already been corrected for this sample shape factor. Furthermore, the experiments have to correspond to the limit of infinite dilution. The average chemical shift of xenon in selected solvents at 298 K and 273 K obtained using the method outlined above are shown in Table V, where they are compared to the experimental values where available.

The average Xe NMR chemical shift resulting from the MD simulations are compared to the experimental spectra shown in Fig. 3. Our MD simulation results give an excellent account of the large difference in the Xe chemical shift of xenon dissolved in water and in perfluorooctyl bromide.

Measurements carried out for Xe in many alkanes over a wide range of temperatures[16] show a linear dependence with temperature and a negative temperature coefficient, that is, the Xe chemical shift is found to decrease with increasing temperature, as seen in three examples given in the third column of Table V. Our MD simulations at 298 K and 273 K for Xe in liquid pentane and hexane (see Table V) uniformly predict that Xe chemical shift in liquid solutions decrease with increasing temperature, that is, we obtain the same sign of the temperature coefficient as was observed experimentally for Xe in these liquids.

It required much longer simulations to obtain good values for the Henry's constant of Xe in the solution. Selected examples are compared with experiment in Table VI.[50] The

TABLE V. Average Xe chemical shifts (ppm) calculated in liquids.

Liquid	Calculated, this work	Observed, with bulk susc. corr.	Reference
$(CH_3)_3CH$ (isobutane)	150±10 (322 K)		
	170±10 (298 K)		
$(CH_3CH_2)_2$ (*n*-butane)	142±5 (350 K)		
	155±10 (298 K)	145.4(23±2 °C)	13
	186±5 (273 K)		
$C(CH_3)_4$ (*neo*-pentane)	175±5 (298 K)		
$CH_3(CH_2)_3CH_3$ (*n*-pentane)	185±10 (298 K)	154.1(23±2 °C)	13
		154.1(25.0±0.3 °C)	8
	215±10 (273 K)	162.2(0±0.3 °C)	16
		−0.362 ppm/K	
		173–303 K	
$CH_3(CH_2)_4CH_3$ (*n*-hexane)	212±15 (298 K)	160.3(23±2 °C)	13
		160.9(25.0±0.3 °C)	8
	225±15 (273 K)	168.6(0±0.3 °C)	16
		−0.314 ppm/K	
		173–323 K	
$CH_3(CH_2)_6CH_3$ (*n*-octane)	220±15 (298 K)	169.8(23±2 °C)	13
		169.9(25.0±0.3 °C)	8
		176.8(0±0.3 °C)	16
		−0.304 ppm/K	
		228–328 K	
$(CF_3)_3CF$	90±5 (298 K)		
$C(CF_3)_4$	75±5 (348 K)		
$CF_3(CF_2)_6CF_3$ (PFO)	78±5 (298 K)		
$CF_3(CF_2)_6CF_2Br$ (PFOB)	105±5 (298 K)	106 (room *T*)	5
H_2O	195±5 (298 K)	196.0(23.5 °C)	11

molar fraction solubility X_1 of xenon in pure water at a pressure of 101.325 kPa is described by the empirical formula[51]

$$\ln(X_1) = -74.7398 + 105.21(T/100\mathrm{K})^{-1} + 27.4664\ln(T/100\mathrm{K})$$

for $273.15\,\mathrm{K} \leqslant T \leqslant 348.15\,\mathrm{K}$, according to which, the molar fraction solubility of xenon in water amounts to only $X_1 = 7.92\times10^{-5}$ at 298 K. Xe has greater solubility in organic solvents such as the alkanes and fluoroalkanes in this study. For example, the solubility of Xe in perfluorooctyl bromide is about 11 times that in water.[5]

IV. DISCUSSION

To understand Xe chemical shifts in infinite dilution in liquid solvents, it is helpful to think of the Xe as being surrounded by a dynamic cage of solvent molecules. Thus, the major determinants of the magnitude of the average chemical shift are (a) the electronic structure of individual solvent molecules, (b) the average size of the cage (free volume available to the Xe atom), (c) the range of free volumes that are sampled over time, and (d) the temperature. The electronic structure of the solvent molecules determines both the Xe shielding response and the potential energy of interaction as a function of configuration. Thus, factor (a) has the same nature for Xe in liquids as for Xe in rigid cages in crystalline materials.

The average size of the solvent cage or free volume [factor (b)] depends on the density of the solution, which in turn is determined by the solvent-solvent interaction potential. The effect of the internal volume of the solvent cage on the average Xe chemical shift is the same as for Xe in rigid cages in crystalline materials. The smaller cage permits a sampling of short Xe-cage atom distances. Since we had previously established that the Xe shielding response is increasingly deshielding (to higher positive chemical shifts) with decreasing distance,[21,22] small cages permit sampling of large chemical shift contributions. This is the basis for the observed correlation between cage internal volume and average Xe chemical shifts for a given electronic structure of cage atoms, as for Xe in silicate cages.

Quantum mechanical calculations reveal that the universal sharp change in the Xe shielding response is decidedly nonlinear with decreasing distance of a neighboring atom.[21,22] This means that the range of cage internal volumes sampled over time [factor (c)] will be important, because even the infrequent sampling of the low end of the range of free volumes can make large contributions to the average Xe chemical shifts.

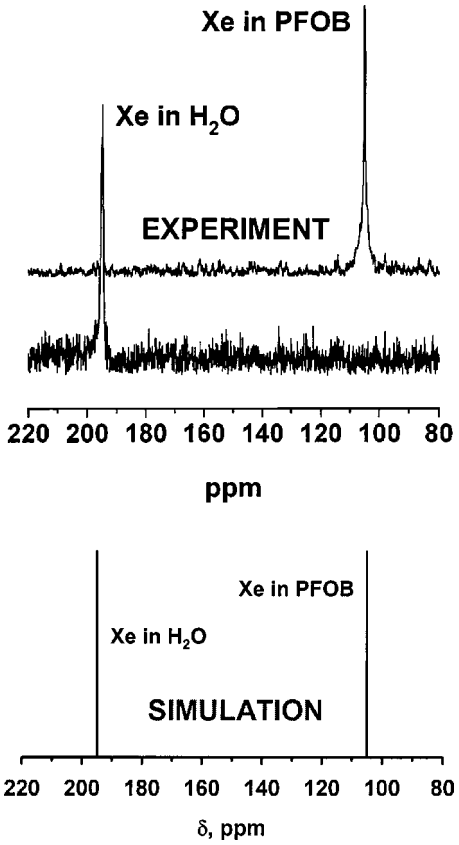

FIG. 3. Xe NMR spectra of Xe at infinite dilution in water and PFOB at room temperature, compared with results of MD simulations. Spectra reproduced from Ref. 5, with permission from Magnetic Resonance in Medicine, Wiley-Liss.

A. Dependence on temperature

Since a linear temperature dependence of the average Xe chemical shift is generally observed for Xe in liquids,[16] the effect of temperature [factor (d)] appears deceptively simple. It is well known that chemical shifts in liquids change with temperature when one is observing a nucleus in the pure solvent. For example, extensive studies of gas to liquid NMR shifts over a wide range of temperatures in simple molecules have established that the ^{19}F chemical shifts varied with temperature, uniformly decreasing as the density of the liquid decreases with increasing temperature.[52–57] The temperature dependence of Xe chemical shifts has been measured in some liquids.[8,16] The MD simulations in the present work provide the theoretical paradigm for the understanding of all such data.

The complexity of the effect of temperature arises from the traditional way in which NMR experiments in liquid solutions are carried out, i.e., at constant pressure, in which case, temperature plays a role in factors (b) and (c) in addition to the effects such as would be observed in the dilute gas phase under constant volume conditions. In the latter simpler system, the sampling of configurations determined by temperature in the factor $\exp[-V/RT]$ gives rise to temperature-dependent Xe chemical shifts under the constant density conditions of a sealed gas sample. Since configurations having short distances between Xe and neighbors give rise to greater Xe shielding response, this intrinsic temperature dependence is decidedly nonlinear.[58] For example, the Xe chemical shifts in $Xe–CH_4$ and $Xe–CF_4$ mixtures at constant density are nonlinear with temperature in theory and experiment.[23] Similarly, in the zero occupancy limit, the average shift for a single Xe in a cage or channel in a crystal has a decidedly nonlinear temperature dependence over a wide temperature range.[59] In contrast, both factors (b) and (c) are affected by temperature in a liquid under the constant pressure conditions of a standard NMR measurement. The density of a liquid typically decreases with increasing temperature and this leads to larger free volumes available to the Xe atom [factor (b)]. Given the sharp dependence of the Xe shielding response on the short distances sampled in the internal volume of the solvent cage, the solvent density change with change in temperature has a significant and dominant contribution to the temperature dependence of the average Xe chemical shift, primarily due to factor (b). This is the primary reason why the average Xe chemical shift in various solvents should not be compared at the same temperature, but rather at a constant reduced temperature, as suggested by Bonifacio *et al.*[16] Furthermore, if the solvent molecules are associating by specific interactions such as hydrogen bonding, then temperature can have unusual effects on the average Xe chemical shift as the disruption of cage-forming hydrogen bonds upon increasing temperature can affect the electronic nature of the neighbors of the Xe atom, in addition to affecting the average geometric configuration of the solvent cage.

In the present MD study of Xe in alkanes, we have kept factor (a) constant so as to explore the role of factors (b), (c), and (d). To establish that factor (b) is the major reason for the temperature dependence of Xe chemical shifts in liquid solutions, we also carried out simulations in which we raised the temperature but maintained the liquid density constant (an MD simulation of the typical high pressure experiments of Jonas[60]). The results are as follows. Raising the temperature of the simulation to 322 K whilst maintaining the density the same as the density at 298 K left the average Xe chemical shift unchanged in isobutane (170 ± 10 ppm). Raising the temperature of the simulation to 350 K while keeping the density of *n*-butane the same as at 298 K also led to no change (155 ± 5 ppm vs 153 ± 5 ppm). These results demonstrate that the change of liquid density with changing temperature is primarily responsible for the temperature dependence of Xe chemical shifts in liquid solvents. With increasing average size of the effective free volume upon increasing temperature dominating the temperature effect on Xe chemical shifts, the temperature dependence of the Xe chemical shift in the limit of infinite dilution in liquid sol-

TABLE VI. Henry's Law constants (atm) for Xe in selected solvents at 298 K.

Solvent	This work	Experiment	Reference
n-butane	56 ± 10		
n-hexane	48 ± 10	40	32
n-octane	48 ± 10	37	32
Water	6000 ± 2000	9500	31

vents is easily predictable: Xe chemical shifts decrease with increasing temperature for a given solvent, primarily due to factor (b). Of course, in those organic solvents where the Xe solubility is significant, the intrinsic temperature dependence of Henry's law constant would bring in the complication of Xe–Xe contributions to the chemical shift, with increased Xe–Xe encounters in higher Xe concentrations. We do not deal with this aspect in the present work.

B. Alkanes versus fluoroalkanes

Our simulations do very well with distinguishing Xe chemical shifts in alkanes compared to perfluoroalkanes, as seen in Table V. The uniformly smaller chemical shifts for Xe dissolved in the fluorinated versions runs counter to the usual idea of higher dispersion contributions from molecules with larger number of electrons. We had found that at the same distance from the C center, the Xe shielding response from a CH_4 molecule is slightly greater than that from a CF_4 molecule for the Xe approach toward the face of the three F or H atoms, whereas the shielding responses at Xe from CH_4 or CF_4 are about the same for approaches along the C–H or C–F bond, or along the bisector to the HCH or FCF angle.[23] The F atom core electrons and the longer C–F bond length do not permit the Xe atom to get as close to the CF_4 as it does to the CH_4 molecule.[23] The differences in the observed Xe chemical shifts in these gas mixtures arise primarily from the averaging; the Xe shielding response is smaller at those distances favored by the Xe–F potential functions. The same holds for the averaging in the MD simulations of Xe chemical shifts in liquid perfluoroalkanes. Thus, for the same number density of C atoms, the Xe chemical shifts in the perfluoroalkanes are smaller than in the alkanes. Our results at room temperature reflect this. There are no published data for Xe in perfluorocarbons, other than CF_4, for comparison with our predictions, although measurements have probably been made in the laboratory of Filipe *et al.*

Our results have some relevance to Xe shifts in polymers. Golemme *et al.* have measured Xe chemical shifts for Xe in glassy perfluorinated polymers that have high free volume.[61] At near-zero loading the Xe chemical shift is 65–84 ppm depending on the polymer. The Xe chemical shifts in these glassy perfluorinated polymers are smaller than those found in polymers with alkyl sidechains.[62] Xe chemical shifts in the voids of polytetrafluoroethylene are found to be about half as large as that found in polycarbonate under the same conditions.[63] These experimental results are entirely consistent with the smaller average chemical shifts that we calculate for Xe in perfluorinated alkyl solvents compared to Xe dissolved in their alkyl counterparts. As we have seen already,[23] both the intrinsic shielding response and the potential functions for Xe–CF_n vs Xe–CH_n lead to a prediction of smaller Xe chemical shifts for Xe–CF_n. Thus, for the same void sizes, Xe in the polymers with pendant CH_n groups should have a larger chemical shift than in the perfluorinated polymers; this is indeed observed experimentally.[61,63,64]

C. Xe in water

The Xe chemical shift in liquid water relative to free Xe atom is found by the MD simulations to be in excellent absolute agreement with experiment; MD simulations give an average Xe chemical shift of 195 ± 5 ppm using the SPC potential for water compared to 196 ppm from experiment.[11] In the present work, MD simulations using TIPS4P gives identical results to those obtained using the SPC potential, within statistical errors. The two liquid water potentials used in this work had been shown to give reasonable agreement with a range of experimental observations on liquid water.[44] Apparently they are both good enough to reproduce the distribution of configurations of water molecules that form transient solvent cages around a Xe atom. In particular, the ability of both liquid water potentials to accurately reproduce the experimental density of liquid water ensures that the liquid structure will provide nearly the correct environment (primarily the correct free volume) for the dissolved Xe atom.

D. Xe in water and perfluorooctylbromide

The ability of Xe to discriminate between biological cavities, in the same chemical shift region as Xe in aqueous solution, and the Xe in the delivery medium is of great advantage in applications of Xe for chemical-shift-selective imaging and spectroscopy, for investigation of cells and tissues *in vivo*.[2] Therefore, we were particularly interested to find out whether it was possible to account for the large Xe chemical shift difference between these two media. The MD simulations give an excellent account of the large difference in Xe chemical shift in water and in PFOB, as can be seen in Fig. 3. The average chemical shifts of Xe in PFOB and H_2O are, respectively, 105 ± 5 and 195 ± 5 ppm, to be compared with the experimental 106 and 196 ppm.

The Xe atom obviously experiences longer average distances from solvent cage atoms in PFOB than in water. That the transient solvent cages in PFOB are much larger than those in liquid water is easy to understand; the smaller molecules tend to form smaller solvent cages than the long extended molecules.

There is a smaller, yet significant, difference between Xe in PFO and PFOB liquids. The two solvent molecules differ only in that one F atom in the former has been replaced by a Br atom. The greater intrinsic shielding response at the Xe from a Br atom, compared to a F atom (a factor of 2.07), will lead to larger average chemical shifts provided the Xe has similar access to the Br atom as to the F atom in that position in PFO. The positions of the center-of-mass in the two molecules are nearly identical; the two molecules PFO and PFOB will generate similar configurations during the MD simulation. With the greater shielding response of Xe to the Br atom, a larger Xe chemical shift in PFOB compared to PFO may be expected. The MD results demonstrate that Xe can tell the difference between the two liquids, resulting in an average Xe chemical shift of 78 ± 5 for PFO, compared to 105 ± 5 for PFOB. With the understanding of the influence of the parameters that determine the average Xe chemical shifts in liquids, especially the perfluoroalkanes that are similar to the compounds already in medical use as oxygen carriers and

blood substitutes, it should be possible to design an alternative to PFOB for the efficient delivery of hyperpolarized xenon to cells and tissues, using as a basis the quantitative insight gained from the present work.

E. Sensitivity to the potential functions used in the simulations

We have not explored other Xe-alkane, Xe-perfluoroalkane potentials since our goal was to demonstrate that it is possible to understand Xe chemical shifts in liquids using the same electronic structure (same shielding and potential functions) as for Xe–CH_4 and Xe–CF_4. Now we consider, in general, the sensitivity of the chemical shift in solutions to the interaction potentials between solute and solvent. Because of the strong dependence of the intermolecular chemical shift on the distance between the nucleus (Xe in our solute example) and the individual atoms of the neighboring solvent molecules, the average chemical shift is sensitive to the Xe-solvent potential over a range of distances typically 3–6 Å. The results of the simulation are sensitive to the Xe-solvent interactions, including the anisotropy of the potential function. Only the isotropic average of the Xe chemical shift can be observed experimentally. However, the shielding response functions are expressed in site-site (Xe–A) form; therefore the MD results are sensitive to the anisotropy of the Xe-solvent potential. Since the greater shielding response is at the shorter distances, the Xe–A potential function has to have a reasonably accurate r_0 and a proper functional behavior for the repulsive region inside of $V=0$. The Lennard-Jones form of Xe–A potential is usually not adequate for this purpose; the r^{-12} form of V is too steep. The temperature dependence is a robust test for the adequacy of the Xe-solvent potential provided the Xe shielding response functions are well described, as is the case for the Xe–C and Xe–H functions we used in this work for alkanes, and the Xe–C and Xe–F functions used for perfluoroalkanes. With a given description of the dynamic liquid structure of the pure solvent, the Xe-solvent interaction parameters may be determined if the shielding response can be calculated quantum mechanically for Xe in the presence of one solvent molecule.

The same reason, the steep dependence of the Xe shielding response on Xe-neighbor distance, makes the average Xe chemical shift in solution also sensitive to the ''free volume'' provided by the dynamic liquid structure. In the present work, we fix the number density of the solvent in the simulation box to be the same as the experimental density, so that the free volume available to the Xe atom in solution is not entirely determined by the accuracy of the solvent-solvent potential; thus, the results of our simulation should not be acutely sensitive to the long range terms in the solvent-solvent potential functions used. We have verified that the average Xe chemical shifts are not extremely sensitive to the details of the solvent-solvent potential, provided the liquid density is reproduced by the potential. For example, upon increasing the parameter r_0 of the CC Lennard-Jones by 2.5% in the MD simulations in isobutane, the average Xe chemical shift remained unchanged within statistical errors, despite the significant increase in the energy of the liquid. As already mentioned, using the SPC or the TIP4P potential for liquid water gave indistinguishable results for the average Xe chemical shift. On the other hand, the sensitivity of the average Xe chemical shift to the liquid density implies that when the individual site-site Xe-solvent interactions are well known (from low-density gas phase chemical shift studies, for example), the solute chemical shift can be used to discriminate between those descriptions of pure liquid solvents that correspond to different densities at a given temperature. This would therefore make the average Xe chemical shift a particularly attractive property for the investigation of complex condensed phases, such as mixtures of liquid solvents or liquid crystals.

We have shown in Table I that the Xe@CH_4 model is not directly transferable to Xe-alkane and that we expect to always overestimate the Xe chemical shifts for alkanes because the Xe chemical shift function for Xe@CH itself varies with increasing C substitution for H. This is part of the reason why the calculated average chemical shifts are overestimates in every case when compared to the experimental values in the alkanes. We note that the deviations become larger as the alkane length increases. Finally, we should note that we have used only rigid molecules in these MD simulations; we have not accounted explicitly for the effect of the torsional degrees of freedom of the solvent molecules on the average Xe chemical shift. Therefore, subtle differences, such as the 2–10 ppm chemical shift differences for Xe in branched alkanes vs normal alkanes cannot be accounted for in the present work. The packing of rigid all-trans molecules is different from the case where a distribution of conformations is allowed. The deviations of the calculated chemical shifts from the experimental values therefore become more pronounced as the number of internal rotation degrees of freedom in the alkane increases. On the other hand, the higher internal moments of inertia of CF_n groups correspond to smaller rotational velocities and the bulkier F atoms compared to H atoms corresponds to higher barriers to internal rotation in the perfluorocarbons. The Br atom is bulkier yet, so neglect of internal rotation in PFOB is not as severe an approximation. Thus, we represent dynamics in the perfluoro solvents more faithfully than the dynamics in the alkanes, with concomitant expectations of better agreement with experiment in the Xe chemical shifts. The predicted Xe chemical shifts in perfluoro alkanes need to be tested experimentally.

V. CONCLUSIONS

We have carried out calculations of Xe chemical shifts in liquids, for the first time. Previous interpretations were primarily empirical correlations between the observed Xe chemical shifts and functions of refractive index of the liquid solvents or semiempirical measures of dispersion energies. The MD simulations in the present work used shielding response and potential functions for Xe which are identical to those used for Xe in gas and crystalline phases; and the liquid-liquid potentials were adopted from standard sources. No parameters were adjusted to chemical shift data. We have shown that this general approach successfully provides good Xe chemical shift averages that are comparable with experi-

ment, reproducing systematic trends in a variety of liquids. We have demonstrated that the magnitudes of the Xe chemical shifts in liquid solutions and the temperature dependence of the shifts can be understood from consideration of Xe in solvent cages. The major difference between the Xe chemical shifts in semirigid cages and channels in our previous work and the Xe chemical shifts in liquid solutions in the present work is that the solvent cages are very dynamic and very temperature dependent in the liquid state. The use of MD simulations, instead of Monte Carlo simulations using an ensemble of static solvent cage structures, ensures that the Xe will average over the proper distribution of instantaneous solvent cage sizes and shapes, as dictated by the structure of the liquid. This molecular level picture of Xe chemical shifts in liquid solvents is therefore entirely consistent with the interpretation of Xe in gas phase mixtures and in rigid cages in crystals. In this way, the present approach is superior to empirical correlations of Xe chemical shifts with dispersion-based quantities.

Correlations of Xe chemical shifts with Xe-solvent dispersion energy or other quantities (such as refractive index) that are related to polarizability or dispersion energy have been shown here to be spurious. Some empirical correlations do appear when considering related compounds since the intermolecular interaction potential is involved in the averaging process, *not that the intrinsic Xe shielding response arises from dispersion or electrical polarization in the reaction field*. Despite the greater polarizabilities of the *n*-perfluoroalkanes compared to *n*-alkanes, the Xe chemical shifts at room temperature are greater in the latter. The intrinsically smaller Xe shielding response to the CF_n group, coupled with the longer r_0 of the Xe–CF_n potential, dictates that the Xe averages over that portion of the Xe shielding response surface which is smaller in magnitude, relative to the CH_n analog, resulting in a smaller average Xe chemical shift.

For Xe dissolved in water, the results of the MD simulations are in excellent agreement with experiment. In contrast to the transferred Xe–C, Xe–H, and Xe–F functions, the Xe shielding response functions used for water had been calculated quantum mechanically in water cages of known structure. The MD average should be correct, provided a reasonably good solvent-solvent potential is used.

Our success in both grand canonical Monte Carlo and MD simulations using site-site shielding and potential functions suggests that we may be able to use this general approach in the prediction of Xe chemical shifts in biological cavities where the pendant functional groups (such as side chains) in the cavities are fluxional.

ACKNOWLEDGMENTS

This research was funded by the National Science Foundation [Grant Nos. CHE-9979259 (C.J.J.) and CTS-0314203 (S.M.)], DOE (Grant No. DE-FG02-96ER14680, S.M.), and the Petroleum Research Fund of the American Chemical Society (S.M.).

[1] A. Cherubini and A. Bifone, Prog. Nucl. Magn. Reson. Spectrosc. **42**, 1 (2003).
[2] B. M. Goodson, J. Magn. Reson. **155**, 157 (2002).
[3] S. D. Swanson, M. S. Rosen, K. P. Coulter, R. C. Welsh, and T. E. Chupp, Magn. Reson. Med. **42**, 1137 (1999).
[4] A. Bifone, Y. Q. Song, R. Seydoux, R. E. Taylor, B. M. Goodson, T. Pietrass, T. Budinger, G. Navon, and A. Pines, Proc. Natl. Acad. Sci. U.S.A. **93**, 12932 (1996).
[5] J. Wolber, I. J. Rowland, M. O. Leach, and A. Bifone, Magn. Reson. Med. **41**, 442 (1999).
[6] J. Wolber, D. J. O. McIntyre, L. M. Rodrigues, P. Camochan, J. R. Griffiths, M. O. Leach, and A. Bifone, Magn. Reson. Med. **46**, 586 (2001).
[7] C. I. Ratcliffe, Annu. Rep. NMR Spectrosc. **36**, 123 (1998).
[8] T. R. Stengle, N. V. Reo, and K. L. Williamson, J. Phys. Chem. **85**, 3772 (1981).
[9] T. R. Stengle, S. M. Hosseini, H. G. Basiri, and K. L. Williamson, J. Solution Chem. **13**, 779 (1984).
[10] T. R. Stengle, S. M. Hosseini, and K. L. Williamson, J. Solution Chem. **15**, 777 (1986).
[11] K. W. Miller, N. V. Reo, A. J. M. S. Uiterkamp, D. P. Stengle, T. R. Stengle, and K. L. Williamson, Proc. Natl. Acad. Sci. U.S.A. **78**, 4946 (1981).
[12] J. H. Walton, J. B. Miller, and C. M. Rolan, Appl. Magn. Reson. **8**, 535 (1998).
[13] Y. H. Lim and A. D. King, J. Phys. Chem. **97**, 12173 (1993).
[14] Y. H. Lim, N. Nugara, and A. D. King, Appl. Magn. Reson. **8**, 521 (1995).
[15] M. Luhmer and K. Bartik, J. Phys. Chem. A **101**, 5278 (1997).
[16] R. P. Bonifacio, E. J. M. Filipe, and T. G. Nunes, XEMAT2000 Proceedings, 28–30 June, 2000, Sestri Levante, Italy.
[17] F. H. A. Rummens, J. Chem. Phys. **72**, 448 (1975).
[18] F. H. A. Rummens, Chem. Phys. Lett. **31**, 596 (1975).
[19] M. Luhmer, A. Dejaegere, and J. Reisse, Magn. Reson. Chem. **27**, 950 (1989).
[20] A. Dejaegere, M. Claessens, M. Bardiaux, M. Luhmer, and J. Reisse, J. Phys. Chem. **92**, 7093 (1988).
[21] A. C. de Dios and C. J. Jameson, J. Chem. Phys. **107**, 4253 (1997).
[22] C. J. Jameson, D. N. Sears, and A. C. de Dios, J. Chem. Phys. **118**, 2575 (2003).
[23] D. N. Sears and C. J. Jameson, J. Chem. Phys. **121**, 2151 (2004).
[24] D. Stueber and C. J. Jameson, J. Chem. Phys. **120**, 1560 (2004).
[25] C. J. Jameson and D. Stueber, J. Chem. Phys. **120**, 10200 (2004).
[26] C. J. Jameson, A. K. Jameson, and S. M. Cohen, J. Chem. Phys. **65**, 3401 (1976).
[27] C. J. Jameson and A. C. de Dios, J. Chem. Phys. **97**, 417 (1992).
[28] S. Murad and S. Gupta, Fluid Phase Equilib. **187–188**, 29 (2001).
[29] S. Murad and S. K. Gupta, Chem. Phys. Lett. **319**, 60 (2000).
[30] M. P. Allen and D. J. Tildesley, *Computer Simulation of Liquids* (Clarendon, Oxford, 1987).
[31] R. P. Kennan and G. L. Pollack, J. Chem. Phys. **93**, 2724 (1990).
[32] G. L. Pollack, J. Chem. Phys. **75**, 5875 (1981).
[33] R. P. Bonifacio, M. F. Costa Gomez, and E. J. M. Filipe, Fluid Phase Equilib. **193**, 41 (2002).
[34] C. M. Colina, A. Galindo, F. J. Blas, and K. E. Gubbins, Proceedings of the 15th Symposium on Thermophysical Properties, Boulder, Colorado, 2003.
[35] C. J. Jameson and S. Murad, Chem. Phys. Lett. **380**, 556 (2003).
[36] C. J. Jameson, A. K. Jameson, P. Kostikin, and B. I. Baello, J. Chem. Phys. **112**, 323 (2000).
[37] R. A. Aziz and A. van Dalen, J. Chem. Phys. **78**, 2402 (1983).
[38] C. McCabe, L. M. B. Dias, G. Jackson, and E. J. M. Filipe, Phys. Chem. Chem. Phys. **3**, 2852 (2001).
[39] R. Friedemann, S. Naumann, and B. Brickmann, Phys. Chem. Chem. Phys. **3**, 4195 (2001).
[40] J. S. Rowlinson, *Cohesion: A Scientific History of Intermolecular Forces* (Cambridge University Press, New York, 2002).
[41] W. L. Jorgensen, J. D. Madura, and C. J. Swenson, J. Am. Chem. Soc. **106**, 6638 (1984).
[42] E. K. Watkins and W. L. Jorgensen, J. Phys. Chem. A **105**, 4118 (2001).
[43] W. L. Jorgensen, J. Chandrasekhar, J. D. Madura, R. W. Impey, and M. L. Klein, J. Chem. Phys. **79**, 926 (1983).
[44] B. Guillot, J. Mol. Liq. **101**, 219 (2002).
[45] J. Schnitker and A. Geiger, Z. Phys. Chem. (Munich) **155**, 29 (1987).
[46] M. Luhmer, D. van Belle, J. Reisse, M. Odelius, J. Kowalewski, and A. Laaksonen, J. Chem. Phys. **98**, 1566 (1993).
[47] M. Odelius, J. Phys. Chem. **98**, 12108 (1994).

[48] M. Luhmer, A. Moschos, and J. Reisse, J. Magn. Reson., Ser. A **113**, 164 (1995).
[49] M. Luhmer and J. Reisse, J. Magn. Reson., Ser. A **115**, 197 (1995).
[50] R. Battino, in *Solubility Data Series*, edited by H. L. Clever (Pergamon, Oxford, 1979), Vol. 2, pp. 133–136.
[51] E. Wilhelm, R. Battino, and R. J. Wilcock, Chem. Rev. (Washington, D.C.) **77**, 219 (1977).
[52] C. J. Jameson, A. K. Jameson, and S. Wille, J. Chem. Phys. **74**, 1613 (1981).
[53] C. J. Jameson, A. K. Jameson, and D. Oppusunggu, J. Chem. Phys. **81**, 85 (1984).
[54] C. J. Jameson and A. K. Jameson, J. Chem. Phys. **81**, 1198 (1984).
[55] C. J. Jameson, A. K. Jameson, and D. Oppusunggu, J. Chem. Phys. **81**, 2571 (1984).
[56] C. J. Jameson, A. K. Jameson, and D. Oppusunggu, J. Chem. Phys. **81**, 2313 (1984).
[57] C. J. Jameson and A. K. Jameson, J. Magn. Reson. **62**, 209 (1985).
[58] C. J. Jameson, Bull. Magn. Reson. **3**, 3 (1980).
[59] A. Labouriau, T. Pietrass, W. A. Weber, B. C. Gates, and W. L. Earl, J. Phys. Chem. B **103**, 4323 (1999).
[60] J. Jonas, Ber. Bunsenges. Phys. Chem. **94**, 307 (1990).
[61] G. Golemme, J. B. Nagy, and A. Fonseca, XEMAT2000 Proceedings, 28–30 June, 2000, Sestri Levante, Italy.
[62] T. Suzuki, M. Miyauchi, M. Takekawa, H. Yoshimizu, Y. Tsujita, and T. Kinoshita, Macromolecules **34**, 3805 (2001).
[63] B. Nagasaka, H. Omi, T. Eguchi, H. Nakayama, and N. Nakamura, Chem. Phys. Lett. **340**, 473 (2001).
[64] Y. Wang, P. T. Inglefield, and A. A. Jones, Polymer **43**, 1867 (2002).